Magnetic and crystallographic properties of $NdMn_{6-x}Fe_xSn_6$ intermetallics

2004 J. Phys.: Condens. Matter 16 5407

(http://iopscience.iop.org/0953-8984/16/30/003)

INSTITUTE OF PHYSICS PUBLISHING JOURNAL OF PHYSICS: CONDENSED MATTER

J. Phys.: Condens. Matter **16** (2004) 5407–5417 PII: S0953-8984(04)77094-0

Magnetic and crystallographic properties of $NdMn_{6-x}Fe_xSn_6$ intermetallics

J Han[1,3], G K Marasinghe[1,2], J B Yang[1,2], W J James[2,3], M Chen[4], W B Yelon[2,3], Ph l'Héritier[5], I Dubenko[6] and N Ali[6]

[1] Graduate Center for Materials Research, University of Missouri-Rolla, Rolla, MO 65409, USA
[2] Department of Physics, University of Missouri-Rolla, Rolla, MO 65409, USA
[3] Department of Chemistry, University of Missouri-Rolla, Rolla, MO 65409, USA
[4] Department of Physics, University of Missouri-Columbia, Columbia, MO 65211, USA
[5] Laboratoire des Matériaus et du Génie Physique, UMR 5628 CNRS, ENSPG, 38402 Saint Martin d'Héres, France
[6] Department of Physics, Southern Illinois University at Carbondale, Carbondale, IL 62901, USA

Received 28 February 2004
Published 16 July 2004
Online at stacks.iop.org/JPhysCM/16/5407
doi:10.1088/0953-8984/16/30/003

Abstract

Intermetallic compounds of $NdMn_{6-x}Fe_xSn_6$ ($0 \leqslant x \leqslant 2.0$) were studied by means of x-ray and neutron diffraction techniques and SQUID magnetic measurements in the temperature range of 30–400 K. The substitution of iron for manganese leads to a phase transition whereby $NdMn_6Sn_6$ with the $HoFe_6Sn_6$ structure (space group *Immm*) changes to $TbFe_6Sn_6$ (space group *Cmcm*) for $NdMn_{6-x}Fe_xSn_6$ with $x \geqslant 0.5$. The iron atoms prefer to occupy the 8g sites at iron content $x < 2.0$ due to the longest Mn/Fe–Sn bond distance. The Curie temperature (T_C) increases from $x = 0$ to 1.5 and then decreases for the larger iron content. The magnetic moment of the iron sublattice couples ferromagnetically with the manganese and neodymium moments for the $x < 2.0$ samples. Spin reorientation is observed in samples with iron content up to 1.5, and the spin reorientation temperature (T_s) increases with increasing iron content. Except for $NdMn_4Fe_2Sn_6$, the easy direction of magnetization for all samples is parallel and perpendicular to the (*bc*) plane of the unit cell at 300 and 30 K, respectively. The easy direction of magnetization for $NdMn_4Fe_2Sn_6$ is parallel to the *a*-axis in the entire temperature range mentioned above, as a result of the anisotropic contraction of the unit cell along the (*bc*) plane.

1. Introduction

Recently, a large number of studies has been devoted to the crystal and magnetic properties of RMn_6X_6 [1–10] (R = rare earth and X is Ge or Sn) intermetallics because the manganese atoms have the potential to possess the largest magnetic moment among the 3d transition metal elements, e.g. $>4.0\ \mu_B$ in Y_6Mn_{23} [11]. The $NdMn_6Sn_6$, $SmMn_6Sn_6$ [4], $NdMn_6Ge_6$ [2, 12],

and $SmMn_6Ge_6$ [2, 13] compounds have received more attention than other intermetallics because not only do they have different crystal structures than those of the others, but one also observes ferromagnetic exchange interaction within and between the rare earth and manganese sublattices in these intermetallics. In these compounds, a spin reorientation was observed in the temperature range of 2–300 K. However, in the above mentioned compounds, theoretically possible large manganese magnetic moments have not been observed. All the RMn_6Sn_6 intermetallics crystallize in either the $HfFe_6Ge_6$ [14] (R = Sc, Y, Gd–Lu) or $HoFe_6Sn_6$-type [4, 15] structures (R = Nd, Sm). Of these intermetallics, only $NdMn_6Sn_6$ and $SmMn_6Sn_6$ display ferromagnetic ordering within and between the rare earth and manganese sublattices. The Curie temperatures of $NdMn_6Sn_6$ and $SmMn_6Sn_6$ are 357 and 405 K, respectively [4]. The other RMn_6Ge_6 intermetallics order either ferrimagnetically or antiferromagnetically [3, 4]. Recent studies of RFe_6Sn_6 (R = Y, Gd–Lu) show that the Fe sublattice orders antiferromagnetically below 480 K and has a strong easy axis anisotropy [16–18]. Therefore, it was of interest to investigate the effect of substituting some Fe for Mn on the exchange interactions (Mn–Mn, Mn–Fe), and the anisotropy of $NdMn_6Sn_6$. A study of the crystallographic, magnetic, and electronic structures of such materials could lead to a better understanding of their magnetic ordering process and anisotropy. In the present study, we have used x-ray and neutron diffraction and SQUID measurements to investigate the crystallographic and magnetic structures of $NdMn_{6-x}Fe_xSn_6$ ($0 \leqslant x \leqslant 2.0$) intermetallics.

2. Experimental procedures

All of the $NdMn_{6-x}Fe_xSn_6$ samples were prepared from elements of purity 99.99% or better by induction melting in a cold boat copper crucible under an argon atmosphere. To ensure homogeneity, the sample ingots were turned over and remelted several times, followed by annealing at 750 °C for two weeks under an argon atmosphere. Six atomic per cent excess manganese was added to compensate for the volatilization of manganese during melting. The phase purity of the samples was checked by x-ray diffraction (XRD) utilizing Cu Kα radiation on a Scintag XDS 2000 diffractometer equipped with a single crystal graphite monochromator. All samples are nearly monophasic, exhibiting less than 2 mol% impurity phase. Samples with $x > 2.0$ were prepared but they contained a larger amount of impurity and therefore were discarded. The bulk magnetic properties, M versus T and M versus H behaviour, were measured with SQUID and VSM. The thermomagnetic data, M versus T, were collected under an applied field of 300 Oe after the samples were magnetized under 2 kOe.

The powder neutron diffraction data were obtained at the University of Missouri Research Reactor for samples placed in thin-walled vanadium containers utilizing neutrons of wavelength 1.4875 Å. Neutron diffraction data were collected at 30 and 300 K for each sample. Crystallographic and magnetic structural parameters were refined by fitting the neutron diffraction data using the Fullprof program [19].

Additional information as to the easy direction of magnetization was obtained by x-ray diffraction studies of samples that were magnetically aligned in-plane. In this procedure, a 325 mesh powder–epoxy mixture placed in an x-ray diffraction sample holder is allowed to harden in a magnetic field of about 10 kOe applied parallel to the sample surface. The applied field forces those crystallographic planes perpendicular to the easy direction of magnetization to preferentially align perpendicular to the sample surface. Similarly, crystallographic planes which are parallel to the easy direction of magnetization will preferentially align, even though to a lesser degree, parallel to the sample surface. Consequently, the relative intensities of reflections in the x-ray diffraction pattern of the magnetically oriented samples will differ from those of the random powder sample.

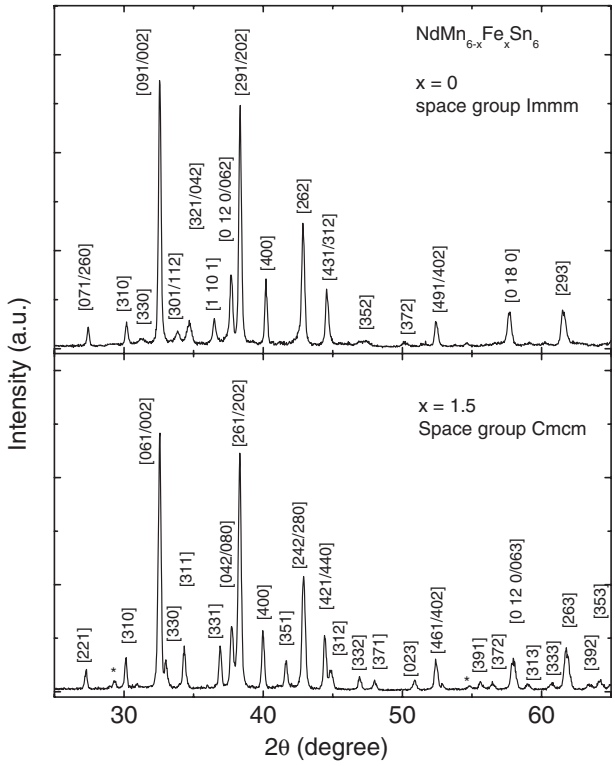

Figure 1. X-ray diffraction patterns of $NdMn_6Sn_6$ and $NdMn_{4.5}Fe_{1.5}Sn_6$ at 300 K (* the peaks of the impurity phase).

3. Results and discussions

The x-ray diffraction (XRD) patterns at room temperature of $NdMn_6Sn_6$ and $NdMn_{4.5}Fe_{1.5}Sn_6$ are shown in figure 1. It is found that the $NdMn_6Sn_6$ and $NdMn_{6-x}Fe_xSn_6$ samples with $0.5 \leqslant x \leqslant 2.0$ crystallized in the $HoFe_6Sn_6$-type (space group *Immm*) and $TbFe_6Sn_6$-type (space group *Cmcm*) structures, respectively. All the characteristic lines match that of $HoFe_6Sn_6$ (*Immm*) and $TbFe_6Sn_6$-type (*Cmcm*) structures reported by Malaman *et al* [4] and Rao *et al* [20], respectively. This is also confirmed by the neutron diffraction data shown in figure 4 where the Fullprof refinement gives a good fit based on these two types of structure.

Figure 2 shows the temperature dependence curves of the magnetization of $NdMn_{6-x}Fe_xSn_6$. The thermomagnetic curve for $NdMn_6Sn_6$ is in good agreement with the work of Malaman *et al* [4] and shows two transitions appearing at approximately 139 and 350 K, respectively. The one at 350 K represents the Curie temperature. The other one at 139 K has been assigned to a spin reorientation as described below. Similar thermomagnetic behaviour was observed for $NdMn_{6-x}Fe_xSn_6$ with $0.5 \leqslant x \leqslant 1.5$, where the spin reorientation temperature (T_s) shifts to the high temperature range as the iron content increases, and disappears at $x = 2.0$. The bulk magnetization curve of $NdMn_4Fe_2Sn_6$ shows no magnetic transition below its Curie temperature of 361 K. The Curie temperature of $NdMn_{6-x}Fe_xSn_6$ increases from $x = 0$ to 1.5 and then decreases as x further increases; see table 1.

Figure 3 is the magnetic field dependence of the magnetization for $NdMn_{6-x}Fe_xSn_6$ at 30 and 300 K. The measured magnetizations are included in table 1. Except for $NdMn_4Fe_2Sn_6$

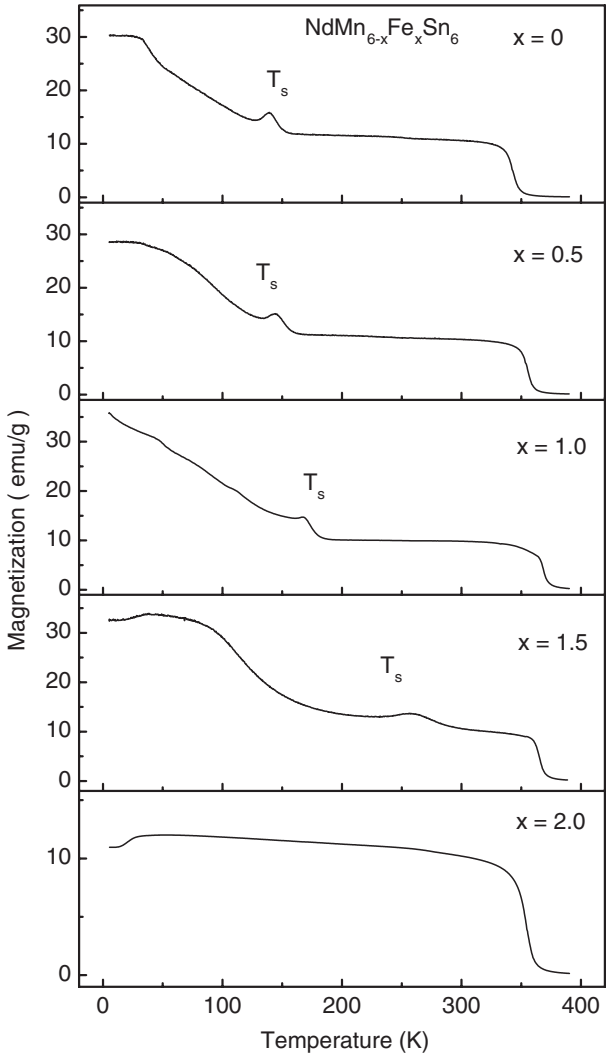

Figure 2. Specific magnetization versus temperature data for $NdMn_{6-x}Fe_xSn_6$ at an applied field of 2 kOe (T_s is the spin reorientation temperature).

at 30 K, the net magnetization of all samples has nearly reached its saturation value when the applied field exceeds 4.0 and 3.0 T for 30 and 300 K, respectively. The net magnetization of all samples at 5.5 T has only a 7% difference in magnitude between the highest and lowest values at room temperature due to the fact that the Curie temperatures of all samples are around 300 K. For sample $NdMn_4Fe_2Sn_6$, the magnetization increases slowly with the applied field at 30 K, suggesting an antiferromagnetic-like behaviour. There is a larger difference drop in the net magnetization at 5.5 T for $NdMn_4Fe_2Sn_6$ as compared to $NdMn_{4.5}Fe_{1.5}Sn_6$ at 30 K, indicating an antiferromagnetic coupling between the magnetic moments of Fe and Mn atoms.

Figure 4 shows the neutron diffraction patterns of $NdMn_6Sn_6$ and $NdMn_{4.5}Fe_{1.5}Sn_6$ at room temperature and 30 K. The data were refined based on the $HoFe_6Sn_6$-type (space group *Immm*) and the $TbFe_6Sn_6$-type [15] (space group *Cmcm*) structures, respectively. Refinements

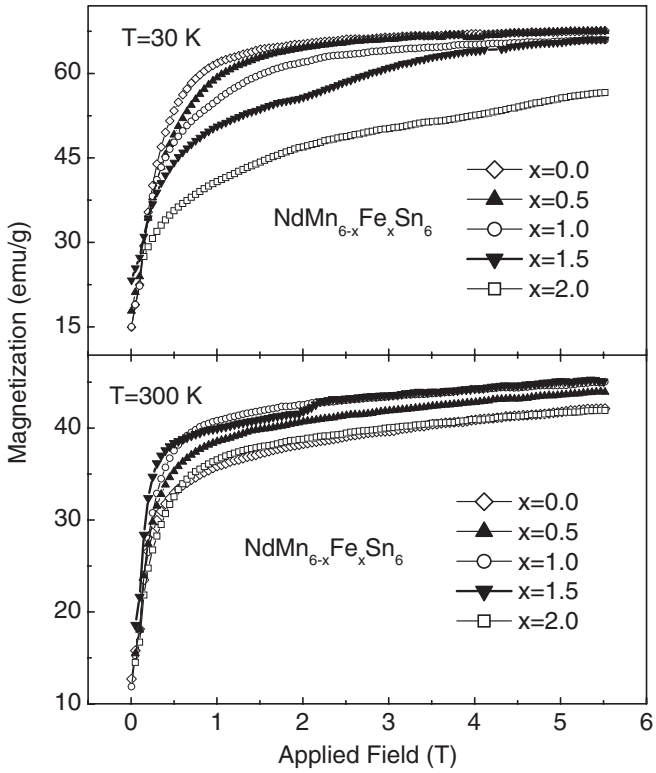

Figure 3. Specific magnetization of $NdMn_{6-x}Fe_xSn_6$ versus applied field at 30 and 300 K.

Table 1. Magnetic properties of $NdMn_{6-x}Fe_xSn_6$ at 30 and 300 K. (Note: T_s is the spin reorientation temperature; T_C is the Curie temperature; M is the magnetic moment per formula unit calculated from the values at a field of 5 T.)

	x				
$NdMn_{6-x}Fe_xSn_6$	0	0.5	1.0	1.5	2.0
T_s (K)	139	146	169	260	—
T_C (K)	350	361	372	372	361
M (μ_B/f.u.) (30 K)	13.8	14.1	14.2	14.4	—
M (μ_B/f.u.) (300 K)	8.96	9.35	9.63	9.49	8.96

yield the lattice parameters, the atomic coordinates and the occupancy factors which are listed in tables 2–4. These two structure types are closely related in that they are both superstructures of the YCo_6Ge_6-type structure [9], where the Sn–R–Sn and R–Sn–Sn–R slabs stack within the hexagonal Mn/Fe–Sn network in different sequences. There is a simple correspondence for the lattice parameters: $a_{Ho} = a_{Tb}$ (∼9 Å); $2b_{Ho} = 3b_{Tb}$ (∼29 Å); $C_{Ho} = C_{Tb}$ (∼5.5 Å) according to [4]. The unit cell contracts slightly with increasing iron content at an average rate of 1.2% per substituted atom, which is due to the fact that the Fe atom has a smaller atomic radius as compared to the Mn atom. The lattice parameter a remains almost constant, while b and c contract at a rate of 0.6% and 0.5% per substituted Fe atom, respectively, indicating that the contraction of the unit cell is anisotropic. The iron occupancies in $NdMn_{6-x}Fe_xSn_6$ ($x \neq 0$) have been refined. As shown in figure 5, the iron atom almost completely avoids the 8e

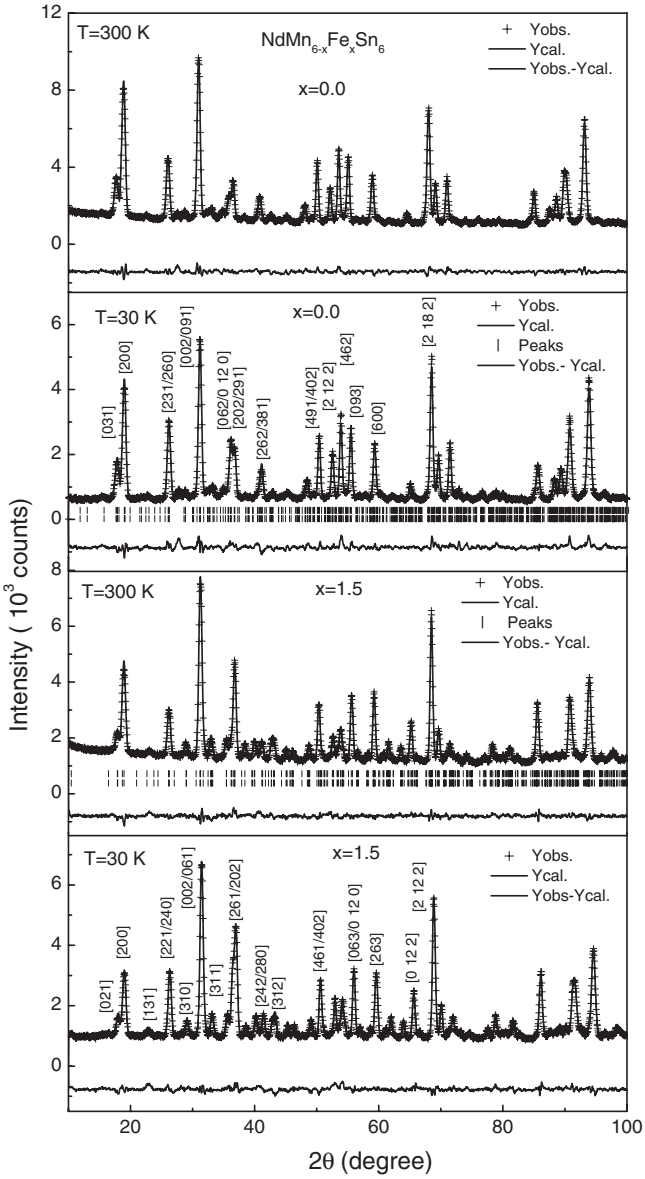

Figure 4. Neutron diffraction patterns of $NdMn_6Sn_6$ and $NdMn_{4.5}Fe_{1.5}Sn_6$ at 30 and 300 K. In the patterns, the bottom curves (Y_{obs}–Y_{cal}) are the difference between experimental and refinement data. The vertical bars indicate the magnetic (bottom) and Bragg (top) peak positions.

sites and prefers the 8g sites at low iron compositions. At compositions of about $x = 2.0$, the iron atom occupies the 8e, 8d, and 8g sites in an approximately random fashion. At low iron content, apparently because of the very short Mn/Fe–Sn bond distance, the iron atom avoids the 8e sites even though this site has the largest Wigner–Seitz atomic volume (V_{wz}) based on Blokje [21] calculations (see table 5). Iron prefers the 8g site due to the longest Mn/Fe–Sn bond distance. This indicates that the preferred occupation of Fe in $NdMn_6Sn_6$ is determined by the Mn/Fe–Sn bond distance in the hexagonal Mn/Fe–Sn network.

Table 2. Lattice parameters for $NdMn_{6-x}Fe_xSn_6$ at 30 and 300 K.

	a (Å)		*b* (Å)		*c* (Å)	
Sample	30 K	300 K	30 K	300 K	30 K	300 K
$NdMn_6Sn_6$	9.0116(5)	9.0581(3)	28.732(5)	28.909(2)	5.5336(9)	5.5765(4)
$NdMn_{5.5}Fe_{0.5}Sn_6$	8.9952(7)	9.0503(5)	19.077(4)	19.202(2)	5.5117(1)	5.5634(5)
$NdMn_{5.0}Fe_{1.0}Sn_6$	9.0119(7)	9.0500(7)	19.029(3)	19.148(3)	5.5113(7)	5.5451(8)
$NdMn_{4.5}Fe_{1.5}Sn_6$	9.0003(4)	9.0382(3)	18.975(1)	19.082(1)	5.4988(4)	5.5333(3)
$NdMn_{4.0}Fe_{2.0}Sn_6$	8.9971(5)	9.0331(4)	18.931(2)	19.042(1)	5.4877(4)	5.5240(3)

Table 3. Atomic sites and occupancy factors (Occ.) of $NdMn_6Sn_6$ at 300 K.

Site	*x*	*y*	*z*	Occ.
Nd(2a)	0	0	0	0.125
Nd(4h)	0	0.1725(3)	1/2	0.25
Mn(4f)	0.2451(21)	0	1/2	0.25
Mn(8k)	1/4	1/4	1/4	0.5
Mn(8n)	0.2479(20)	0.3333(9)	1/2	0.5
Mn(16o)	0.2508(8)	0.0836(6)	0.2573(38)	1.0
Sn(4e)	0.3503(17)	0	0	0.25
Sn(4g)	1/2	0.0538(6)	1/2	0.25
Sn(4g)	0	0.1131(6)	0	0.25
Sn(4g)	0	0.2234(6)	0	0.25
Sn(4h)	0	0.0553(6)	1/2	0.25
Sn(4h)	1/2	0.1131(6)	0	0.25
Sn(4h)	1/2	0.2204(6)	0	0.25
Sn(8n)	0.3349(9)	0.1647(3)	1/2	0.5

Table 4. Atomic sites and occupancy factors (Occ.) of $NdMn_{4.5}Fe_{1.5}Sn_6$ at 300 K.

Site	*x*	*y*	*z*	Occ.
Nd(4c)	0	0.1281(5)	1/4	0.25
Mn(8d)	1/4	1/4	0	0.401
Fe(8d)	1/4	1/4	0	0.099
Mn(8e)	0.2484(34)	0	0	0.384
Fe(8g)	0.2484(34)	0	0	0.116
Mn(8g)	0.2665(42)	0.0929(13)	3/4	0.354
Mn/Fe(8g)	0.2665(42)	0.0929(13)	3/4	0.146
Sn(4c)	0	0.0424(6)	3/4	0.25
Sn(4c)	1/2	0.0408(6)	3/4	0.25
Sn(4c)	0	0.2120(6)	3/4	0.25
Sn(4c)	1/2	0.2051(6)	3/4	0
Sn(8g)	0.3380(3)	0.1248(4)	1/4	0.25

The refinement of the magnetic structure of the $NdMn_{6-x}Fe_xSn_6$ samples was based on the collinear magnetic structure proposed by Malaman *et al* [4] for $NdMn_6Sn_6$. According to this model, neodymium and manganese magnetic moments are ferromagnetically coupled at temperatures between 2 K and the Curie temperature. The manganese and iron moments were refined as an average value. The refined Nd moments of some samples at 30 K were about 4.0 μ_B, markedly higher than the free ion value of 3.0 μ_B found in the normal intermetallic compounds. Furthermore, the refined Nd moments were relatively insensitive to the variation of

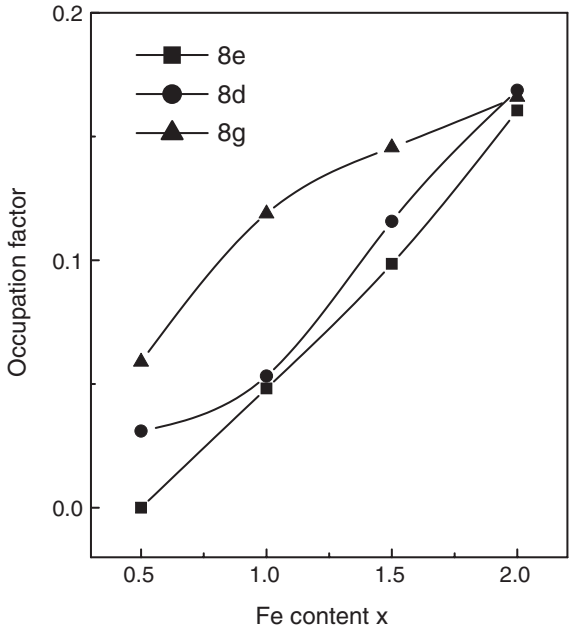

Figure 5. The occupation factors of the Fe atoms on each of three crystallographic Mn sites in $NdMn_{6-x}Fe_xSn_6$.

Table 5. The local environments of Nd and Mn/Fe sites in $NdMn_{4.5}Fe_{1.5}Sn_6$ at 300 K. The atomic radii of Nd, Mn, Fe, and Sn are 1.82, 1.35, 1.27 and 1.55 Å, respectively. The weighted average radius of Mn and Fe was used for the Mn/Fe sites. V_{wz} is the Wigner–Seitz atomic volume.

	Number of near-neighbours			Average distance (Å)			
	Nd	Mn/Fe	Sn	Nd	Mn/Fe	Sn	V_{wz} (Å^3)
Nd(4c)	0	12	8	—	3.5589	3.1702	31.1043
Mn/Fe(8e)	2	4	6	3.6399	2.7877	2.7923	14.1230
Mn/Fe(8d)	2	4	6	3.5155	2.7382	2.8037	13.8369
Mn/Fe(8g)	2	4	6	3.5214	2.7593	2.8122	14.0117

other parameters, likely due to the complex magnetic structure and large number of parameters. Accordingly, the magnetic moment of Nd was fixed to 3.0 μ_B at 30 K according to the previous studies [4]. The refined parameters are listed in table 6. The magnetic moment of Fe/Mn increases from 2.49 μ_B for $x = 0$ to 2.90 μ_B for $x = 1.5$, then decreases to 2.55 μ_B for $x = 2.0$ at $T = 30$ K. At room temperature, the magnetic moment of the Nd atom decreases from 1.59 μ_B $NdMn_6Sn_6$ to 0.75 μ_B for $NdMn_4Fe_2Sn_6$, and the Fe/Mn moment increases from 1.67 μ_B for $NdMn_6FeSn_6$ to 2.09 μ_B for $NdMn_5Fe_1Sn_6$, and then decreases to 1.88 μ_B for $NdMn_4Fe_2Sn_6$. The Fe/Mn magnetic moments do not change linearly with Fe content x, indicating that the low concentration of Fe substitution may enhance the ferromagnetic exchange interactions between Fe/Mn–Fe/Mn by slightly changing the Fe/Mn–Fe/Mn bond length. At a higher Fe composition, a weaker exchange interaction between Fe/Mn–Fe/Mn appears, due to the much shorter bond length, which decreases the Fe/Mn magnetic moments. These effects also lead to the magnetic ordering temperatures showing a nonlinear dependence

Table 6. Refined magnetic properties for $NdMn_{6-x}Fe_xSn_6$ at 30 and 300 K. χ^2 is $[R_{wp}/R_{exp}]^2$; R_{mag} is the R-factor of the magnetic reflections; R_B is the R-factor of the Bragg reflections; φ_a is the angle between the a-axis and the net magnetic moment.

	x				
	0	0.5	1.0	1.5	2.0
	$T = 30$ K				
Nd (μ_B)	3.00[a]	3.00[a]	3.00[a]	3.00[a]	3.00[a]
Mn/Fe (μ_B)	2.49(5)	2.94(6)	2.69(4)	2.90(3)	2.55(4)
φ_a (deg)	16(2)	11(3)	27(2)	15(2)	15(2)
R_B (%)	6.65	7.93	5.69	5.85	7.56
R_{mag} (%)	9.49	10.6	11.8	7.93	9.96
χ^2 (%)	3.56	2.09	4.31	2.40	1.61
	$T = 300$ K				
Nd (μ_B)	1.59(10)	1.58(12)	1.71(13)	1.54(8)	0.75(9)
Mn/Fe (μ_B)	1.67(4)	1.78(5)	2.09(5)	1.96(2)	1.88(3)
φ_a (deg)	90.0	66(3)	61(5)	56(1)	13(3)
R_B (%)	3.94	6.20	6.72	3.73	6.29
R_{mag} (%)	5.12	8.12	8.74	6.30	9.37
χ^2 (%)	2.95	4.05	3.97	1.48	1.90

[a] Magnetic moment of Nd was fixed to 3.0 μ_B at 30 K.

on Fe content. At room temperature, the angle between the a-axis (c-axis of the hexagonal YCo_6Ge_6 subcell) and the moment vector decreases from 90° to 13° as the Fe content increases from $x = 0$ to 2.0. The easy direction of magnetization in $NdMn_6Sn_6$ is almost perpendicular to the a-axis at room temperature and is aligned along the a-axis when the temperature drops below the spin reorientation temperature (T_s) 139 K in agreement with Malaman *et al* [4]. The easy direction in the other samples, except that of $NdMn_4Fe_2Sn_6$, changes from being nearly in the (bc) plane (basal plane of the hexagonal YCo_6Ge_6 subcell) to the a-axis when the temperature falls below the spin reorientation temperature (T_s). The easy direction of magnetization for $NdMn_4Fe_2Sn_6$ is nearly along the a-axis over the temperature range from 30 K to T_C, in agreement with thermomagnetic data. The magnetocrystalline anisotropy of the $NdMn_6Sn_6$ compounds arises from the competition between the magnetic contributions from the Nd and Mn sublattices. The contraction of the unit cell along the b- and c-axes (basal plane of the YCo_6Ge_6 hexagonal subcell) as Mn atoms are substituted by smaller Fe atoms increases the a-axis (c-axis of the YCo_6Ge_6 hexagonal subcell) anisotropy of the Mn/Fe and Nd sublattices, and leads to a-axis anisotropy in $NdMn_4Fe_2Sn_6$. This is consistent with the disappearance of the spin reorientation in $NdMn_4Fe_2Sn_6$. The difference between the orientation of the easy directions of $NdMn_{6-x}Fe_xSn_6$ ($x = 0$ and 2.0) is further confirmed by x-ray diffraction data for magnetically aligned powders. Figure 6 presents the XRD patterns of the random and magnetically aligned powders of $NdMn_{6-x}Fe_xSn_6$ ($x = 0$ and 2.0). The relative intensities of the (400) reflection for the aligned $NdMn_6Sn_6$ samples are considerably larger than those for the non-aligned samples. This indicates that the net magnetic moments of the $NdMn_6Sn_6$ unit cells are close to being perpendicular to the (bc) plane. On the other hand, the relative intensity of the (061) reflection for the aligned $NdMn_4Fe_2Sn_6$ sample is considerably larger than that for the non-aligned sample, indicating its easy direction is along the a-axis.

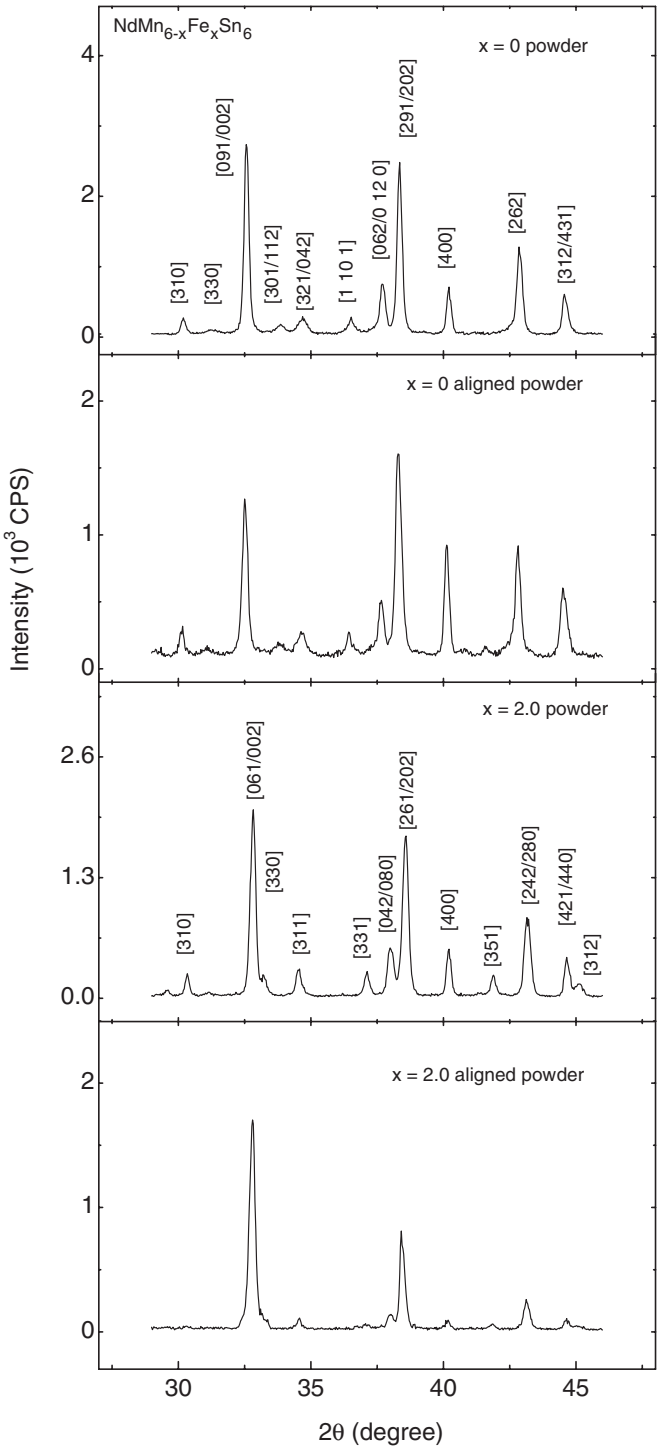

Figure 6. X-ray diffraction data measured at 300 K for random and magnetically aligned powders of $NdMn_{6-x}Fe_xSn_6$ ($x = 0$ and 2.0).

4. Conclusions

The substitution of iron for manganese leads to a phase transition whereby $NdMn_6Sn_6$ with the $HoFe_6Sn_6$ structure (space group *Immm*) changes to $TbFe_6Sn_6$ (space group *Cmcm*) for $NdMn_{6-x}Fe_xSn_6$ with $x \geqslant 0.5$. The iron atoms prefer to occupy the 8g sites at low iron content due to the longest Mn/Fe–Sn bond distance. The unit cell volume decreases anisotropically with increasing iron content, which increases the a-axis anisotropy of the compound. The net magnetization changes very little with increasing iron content. The magnetic moment of the iron sublattice couple ferromagnetically with magnetic moments of the manganese and neodymium sublattices for $x < 2.0$. Except for $NdMn_4Fe_2Sn_6$, the easy direction of all the samples is approximately parallel to the (bc) plane at room temperature, whereas the easy direction is along the a-axis at 30 K.

Acknowledgments

The financial support of the National Science Foundation (grant DMR-9614596) and that of the Defense Advanced Research Projects Agency (grant DAAG 55-98-1-0267) is acknowledged. The SQUID measurements were partially funded by the Materials Technology Center, SIUC.

References

[1] Venturini G, Welter R and Malaman B 1993 *J. Alloys Compounds* **200** 51
[2] Chafik El Idrissi B, Venturini G and Malaman B 1994 *J. Alloys Compounds* **215** 187
[3] Malaman B, Venturini G and Roques B 1988 *Mater. Res. Bull.* **23** 1629
[4] Malaman B, Venturini G, Chafik El Idrissi B and Ressouche E 1997 *J. Alloys Compounds* **252** 41
[5] Lefevre C and Venturini G 2002 *J. Alloys Compounds* **340** 340
[6] Mazet T, Tobola J, Venturini G and Malaman B 2002 *Phys. Rev.* B **65** 104406
[7] Clatterbuck D M and Gschneidner K A Jr 1999 *J. Magn. Magn. Mater.* **207** 78
Clatterbuck D M and Gschneidner K A Jr 1999 *J. Magn. Magn. Mater.* **195** 639
[8] Malaman B, Venturini G, Welter R, Sanchez J P, Vulliet P and Ressouche E 1999 *J. Magn. Magn. Mater.* **202** 519
[9] Venturini G, Fruchart D and Malaman B 1996 *J. Alloys Compounds* **236** 102
[10] Brabers J H V, Zhou G F, Colpa J H P, Buschow K H J and de Boer F R 1994 *Physica* B **202** 1
[11] Hardman K, James W J and Yelon W B 1978 *The Rare Earths in Modern Science and Technology* ed G J McCarthy and J J Rhyne (New York: Plenum) p 403
[12] Han J, Marasinghe G K, James W J, Chen M, Yelon W B, Dubenko I and Ali N 2000 *J. Appl. Phys.* **87** 5281
[13] Han J, Marasinghe G K, James W J, Chen M, Yelon W B, l'Héritier Ph, Dubenko I and Ali N 2000 *IEEE Trans. Magn.* **36** 3324
[14] Olenitch R R, Akselrud L G and Yarmoliuk Ya P 1981 *Dopov. Akad. Nauk Ukr. RSR* A **2** 84
[15] Chafik El Idrissi B, Venturini G and Malaman B 1991 *Mater. Res. Bull.* **26** 1331
[16] Rao X and Coey J M D 1997 *J. Appl. Phys.* **81** 5181
[17] Cadogan J M and Ryan D H 2001 *J. Alloys Compounds* **326** 166
[18] Mazet T and Malaman B 2000 *J. Magn. Magn. Mater.* **219** 33
[19] Rodriguez-Carvajal J 1998 Computer code *Fullprof* Version 3.0.0, Laboratoire Leon Brillouin, France
[20] Rao X L and Coey J M D 1997 *J. Appl. Phys.* **81** 5181
[21] Gelato L 1981 *J. Appl. Crystallogr.* **14** 151